Double-charge-transfer spectroscopy of O_2^{2+}: Band analyses of low-lying repulsive states

Osamu Furuhashi,* Tohru Kinugawa, Takato Hirayama,† and Tetsuo Koizumi†
Research Center for Measurement in Advanced Science, Rikkyo University, Toshima, Tokyo 171-8501, Japan

Chikashi Yamada and Shunsuke Ohtani
Institute for Laser Science, The University of Electro-Communications, Chofu, Tokyo 182-8585, Japan
(Received 24 May 2004; published 4 November 2004)

The double-charge-transfer (DCT) spectrum of O_2^{2+} has been recorded at 140 meV resolution using 1.5 keV H^+ projectiles. Electronic bands of the low-lying triplet states, namely $A\ ^3\Sigma_u^+$, $W\ ^3\Delta_u$, $B\ ^3\Pi_g$, and $B'\ ^3\Sigma_u^-$, have been resolved. Assuming that the observed bands directly reflect the Franck-Condon (FC) profiles, potential-energy curves of the $A\ ^3\Sigma_u^+$, $W\ ^3\Delta_u$, and $B'\ ^3\Sigma_u^-$ states within the FC region are determined based on the reflection approximation. For a quantitative check of the results, complete active space self-consistent-field and multireference configuration-interaction calculations have been performed to predict the potential-energy curves and the FC profiles. The calculated energy curves agree well with the experimentally derived ones. The theoretical FC profiles reproduced well the band shapes observed by both present DCT and previous Doppler-free kinetic-energy release methods. However, our results cast doubt on the previous assignment of luminescence to the O_2^{2+} $B\ ^3\Pi_g \rightarrow A\ ^3\Sigma_u^+$ transition and the observed bound level of the $A\ ^3\Sigma_u^+$ state by the previous threshold photoelectron coincidence experiment.

DOI: 10.1103/PhysRevA.70.052501 PACS number(s): 33.15.Ry, 33.70.Ca, 31.50.Df, 34.70.+e

I. INTRODUCTION

Doubly charged molecular ions (dications) have received considerable attention during recent years [1]. A characteristic feature of diatomic dications is that their potential-energy curves show a shallow well separated from the dissociation limit by a potential barrier. The shallow potential minimum often supports several quasibound vibrational levels located well above the dissociation continuum. Upon dissociation of the molecules in these quasibound states, the bond energy is converted into the kinetic energy of fragment ions; this makes dications interesting as possible systems for energy storage [2]. In order to exploit dications for such purposes, extensive and systematic information on the spectroscopy of these ions is indispensable.

The O_2^{2+} dication, which is of particular importance in ionosphere physics [3], has been studied with a large variety of spectroscopic methods, such as Auger electron spectroscopy [4], double-charge-transfer (DCT) spectroscopy [5], translational energy-loss spectroscopy [6], photoion-photoion coincidence spectroscopy [7], and photoelectron-photoelectron coincidence spectroscopy [8]. These techniques have identified the electronic states of O_2^{2+}, however the results are in poor agreement with each other and with theoretical predictions. Considerable progress has been made in the past decade with the advent of sophisticated techniques, namely threshold photoelectron coincidence (TPESCO) spectroscopy [9] and Doppler-free kinetic-energy release (DFKER) spectroscopy [10]. These techniques have made it possible to resolve vibrational levels and deepened our understanding of O_2^{2+}. Hall *et al.* [9] observed vibrational progression of the ground $X\ ^1\Sigma_g^+$ state by TPESCO spectroscopy and determined molecular constants of this electronic state. This study was later extended by Dawber *et al.* [11] to include excited states. On the other hand, Lundqvist *et al.* [10] measured the kinetic energies released via Coulomb explosion of O_2^{2+} with the DFKER method. Up to now, the DFKER method has provided the best experimental spectrum of O_2^{2+} excited states at excellent resolution (40–60 meV). The vibrational progressions of the $W\ ^3\Delta_u$, $B'\ ^3\Sigma_u^-$, $1\ ^1\Sigma_u^-$, $1\ ^1\Delta_u$, $B\ ^3\Pi_g$, $1\ ^1\Pi_g$, and $1\ ^5\Sigma_u^-$ states were clearly observed. The same authors also performed the complete active space self-consistent-field (CASSCF) and multireference configuration-interaction (MRCI) calculations, and the dissociation mechanism of O_2^{2+} has also been clarified.

With all these achievements, however, a controversial issue regarding the stability of the first-excited $A\ ^3\Sigma_u^+$ state remains unresolved. Tohji *et al.* [12] observed dispersed luminescence following core electron excitation of O_2 by monochromatic synchrotron radiation. The longer-wavelength series matches the known fluorescence of O_2^+, while the shorter-wavelength series, with peaks at 2.97, 2.80, and 2.64 eV, does not match any known luminescence of O_2^+, or other possible atomic or molecular products. Based on the theoretical calculations [13], the same authors have proposed that this unidentified series could be assigned to the $B\ ^3\Pi_g \rightarrow A\ ^3\Sigma_u^+$ transition of O_2^{2+}. In order to observe such luminescence, both the $B\ ^3\Pi_g$ and $A\ ^3\Sigma_u^+$ states should be bound. Later, this assignment was experimentally supported; a single peak at 41.3 eV in the TPESCO spectrum [11] has been assigned to the $A\ ^3\Sigma_u^+$ state, which is weakly bound supporting one vibrational level. On the contrary, high-level CI calculations [10,14] conflict with the above-mentioned observations, predicting that the $A\ ^3\Sigma_u^+$ state is purely dissociative. To give an unambiguous answer to the question of

*Electronic address: furuhasi@rikkyo.ne.jp
†Also at Department of Physics, Rikkyo University, Toshima, Tokyo 171-8501, Japan.

whether the emission observed by Tohji *et al.* is due to the $B\ ^3\Pi_g \rightarrow A\ ^3\Sigma_u^+$ transition, further experimental investigations of O_2^{2+} are still needed.

Recently, we have improved the energy resolution of DCT spectroscopy to resolve vibrational levels of dications ($\leqslant$200 meV). In comparison with other methods at vibrational resolution, this method has the following advantage: direct comparison between the experimental and theoretical spectrum may be possible by virtue of the apparent propensity rules underlying the DCT process, i.e., the spin-conservation rule and the Franck-Condon (FC) principle. The validity of these propensity rules has been confirmed and the unique opportunity of DCT spectroscopy to study molecular dications has been demonstrated for N_2^{2+}, CO^{2+} [15], and NO^{2+} [16].

In this article, we report DCT spectroscopy of O_2^{2+} at an energy resolution of 140 meV. The electronic bands of the low-lying triplet states, namely $A\ ^3\Sigma_u^+$, $W\ ^3\Delta_u$, $B\ ^3\Pi_g$, and $B'\ ^3\Sigma_u^-$, have been resolved. By analyzing the observed band shapes based on the reflection approximation, potential-energy curves of the $A\ ^3\Sigma_u^+$, $W\ ^3\Delta_u$, and $B'\ ^3\Sigma_u^-$ states within the FC region are experimentally determined. This is an attempt to obtain information on dicationic potential-energy curves by analyses of a continuous spectrum. For a quantitative check of the results, full valence CASSCF-MRCI calculations have been performed using a larger basis set to predict the potential-energy curves. The theoretical potential-energy curve of the $A\ ^3\Sigma_u^+$ state is identical to the experimentally derived one, casting doubt on the previous assignment of luminescence to the $O_2^{2+}\ B\ ^3\Pi_g \rightarrow A\ ^3\Sigma_u^+$ transition.

II. EXPERIMENT

The principle of DCT spectroscopy is simple [17]. Incident H^+ projectiles, having 1.5 keV kinetic energy in the present experiment, capture two electrons simultaneously from the target molecule,

$$H^+ + O_2 \rightarrow H^- + O_2^{2+}. \quad (1)$$

From the translational energy loss ΔE of the H^- products scattered towards almost 0°, the double ionization energies $\mathcal{I}_2$ of O_2 are uniquely determined by conservation of the energy and momentum by use of the formation energy of −14.352 eV from H^+ to H^-,

$$\mathcal{I}_2 = \Delta E + 14.352\ \text{eV}. \quad (2)$$

Actually, H^- are also produced via two-step collisions (TSC),

$$H^+ + O_2 \rightarrow H + O_2^+ \quad (3)$$

and

$$H + O_2 \rightarrow H^- + O_2^+. \quad (4)$$

However, the DCT signals are easily distinguished from the TSC ones by varying the target pressure; the DCT signals are linearly dependent on the gas pressure, while the TSC signals exhibit quadratic dependence.

In the present experiment, DCT spectra were obtained by use of two hemispherical electrostatic deflectors having 254 mm mean diameter, one for selecting the energy of H^+ projectiles and the other for analyzing the H^- products. Details of the apparatus are described elsewhere [16]. By using this energy selector, the resolution in the present work has been much improved in comparison with the previous DCT spectrum [5]; the overall instrumental resolution of the present experiment was about 140 meV (full width at half maximum) as estimated from the measured width of argon peaks. The scale of the translational energy loss was calibrated with the DCT peaks of $Ar^{2+}(^1D_2)$ 45.126 eV and $Ar^{2+}(^1S_0)$ 47.514 eV [18]. The overall uncertainty in the peak positions was estimated to be ±50 meV, including statistical errors.

III. THEORY

For a quantitative check of the experimental results, we have performed *ab initio* calculations with the full valence CASSCF-MRCI method using the MOLPRO program package [19]. It has been regarded that a MRCI calculation based on the full valence CASSCF wave function is a minimum requirement for calculating an accurate potential-energy function of a dication. In general, a larger basis set improves accuracy at the expense of computation time. In order to know the effect of the basis-set truncation on the results, we have used three different basis sets, namely the augmented correlation-consistent polarized valence double-zeta, triple-zeta, and quadruple-zeta basis sets of Dunning and coworkers [20], denoted aug-cc-pVDZ, -pVTZ, and -pVQZ, respectively. All the results include the Davidson correction [21] in order to consider the size consistency.

The observed electronic bands are first assigned by reference to theoretical vertical transition energies, defined as a difference of single point energies between the ground $X\ ^3\Sigma_g^-$ state of O_2 and the corresponding dicationic one at the equilibrium distance of neutral O_2 (R_0=1.207 52 Å [22]). Potential-energy curves of O_2^{2+} were also computed to compare with the curves experimentally derived and to obtain the FC profiles. The smooth potential-energy curves were constructed by interpolating *ab initio* energies at 42 nuclear distances from 0.9 to 2.8 Å.

For comparison with the experimental band shapes, we have calculated the theoretical FC profiles using the wave-packet method [23], as in the case of N_2^{2+}, CO^{2+} [15], and NO^{2+} [16]. This method has two major advantages. First, accurate results are given even for strongly anharmonic potential-energy curves, which may allow dissociations via tunneling effects. Second, both the bound and dissociative states are strictly treated within the same framework. These advantages are of practical importance for the present study because most of the O_2^{2+} triplet states are weakly bound or dissociative showing strongly anharmonicity, as we will see later. The computational procedure starts by numerically solving the time-dependent Schrödinger equation with the split-operator fast-Fourier-transform algorithm [24]. An initial wave packet (the v=0 vibrational function of the O_2 ground state) was put on a dicationic potential-energy curve at the equilibrium distance of O_2 (R_0=1.207 52 Å). The autocorrelation function is obtained in the time domain from

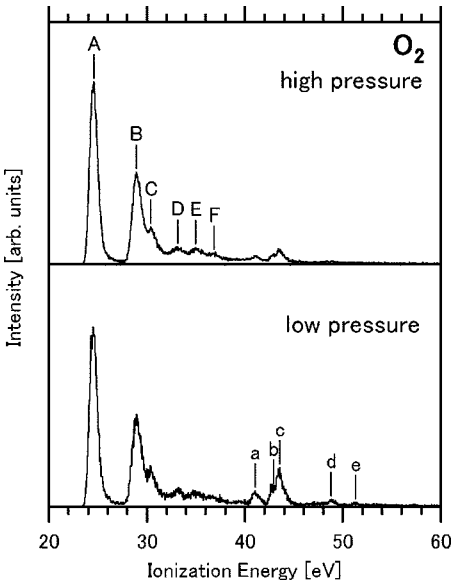

FIG. 1. DCT spectra with different pressures of O_2 using 1.5 keV H^+ projectiles.

the overlap integral between the initial wave packet and the time-propagated wave packet on the dicationic potential-energy curve. This autocorrelation function is then multiplied by an appropriate Gaussian function in the time domain. By Fourier transformation of the autocorrelation function thus modified, we obtain the FC profiles including assumed Gaussian instrumental resolution in the energy domain.

IV. RESULTS AND DISCUSSION

A. Overview of DCT spectra

In order to distinguish the DCT signals from the TSC ones, the wide-range spectra were first measured at a moderate energy resolution ($\approx$0.5 eV) by varying the pressure of the target gas. The results are shown in Fig. 1. In this figure, the target gas pressure of the upper spectrum was nearly double that of the lower one. The accumulation time was 30 min for the upper spectrum and 60 min for the lower one. From the pressure dependence of the signal intensities, the peaks labeled by lowercase letters are due to the DCT process and those labeled by uppercase letters are due to the TSC process.

The electronic bands of the DCT peaks can be assigned in a straightforward manner, using the propensity rules underlying the DCT process. The triplet contributions are expected to be predominant in the observed spectra due to the spin-conservation rule, since the spin-orbit interaction should be weak for a light atom like oxygen. Furthermore, band maxima in the spectra are likely found around the vertical transition energies according to the FC principle. In Table I, the theoretical results of the vertical transition energies for the O_2^{2+} triplet states are summarized, together with the present and previous DCT observations. In this table, all the electronic states below 55 eV are listed. According to the table, the peaks (a) and (b) in Fig. 1 are assigned to the $A\ ^3\Sigma_u^+$ and $W\ ^3\Delta_u$ states, respectively, while the peak (c) can be attributed to the population of both the $B\ ^3\Pi_g$ and $B'\ ^3\Sigma_g^-$ states. The peak (d) is an unresolved mixture of four electronic states as shown in Table I. Possibly the contribution of the $C\ ^3\Pi_u$ state is dominant because in the DFKER spectrum [10] only this electronic state was seen with a peak at 48.897 eV, which agrees with the present observation. A weakly traceable peak (e) can be attributed to the composition of four electronic states, however further assignment is not possible because there was no counterpart around this energy region in both the DFKER [10] and TPESCO [11] spectra.

TABLE I. Vertical transition energies of the O_2^{2+} triplet states in eV.

State	Theory[a]	Experiment[b]	Experiment[c]
$A\ ^3\Sigma_u^+$	40.798	(a) 41.1±0.1	41.1±0.2
$W\ ^3\Delta_u$	42.611	(b) 42.9±0.1	
			43.2±0.2
$B\ ^3\Pi_g$	43.137	(c) 43.4±0.1	
$B'\ ^3\Sigma_g^-$	43.745		
$1\ ^3\Delta_g$	47.529	(d) 48.8±0.1	48.2±0.3
$C\ ^3\Pi_u$	48.310		
$2\ ^3\Pi_u$	48.566		
$1\ ^3\Sigma_g^-$	49.089		
$3\ ^3\Pi_u$	49.934	(e) 51.2±0.2	51.3±0.5
$^3\Pi_u$	50.904		
$^3\Pi_u$	51.404		
$2\ ^3\Sigma_g^-$	51.707		
$^3\Sigma_u^+$	52.675		
$^3\Sigma_g^+$	52.892		
$^3\Pi_g$	52.976		
$^3\Delta_g$	53.163		
$^3\Sigma_g^-$	53.311		
$^3\Pi_g$	53.903		

[a]Using aug-cc-pVTZ basis set.
[b]Present DCT results.
[c]Previous DCT results by Fournier *et al.* [5].

B. Band analyses of the DCT spectrum

With improved energy resolution the DCT spectrum of O_2^{2+} has been recorded, as shown in Fig. 2(a). For this spectrum the H^- signals were accumulated for about 100 min and the background TSC signals were not subtracted. Comparing with the spectrum shown in Fig. 1, a new DCT feature, which can be attributed to the $B'\ ^3\Sigma_u^-$ state, is resolved.

The prominent peak at 43.514±0.050 eV in Fig. 2(a) is the $B\ ^3\Pi_g\ v=0$ level. This assignment is completely consistent with the TPESCO data by Dawber *et al.*, who reported the peak position to be 43.550±0.010 eV. According to the theoretical calculation of Lundqvist *et al.* [10], the potential-energy curve of the $B\ ^3\Pi_g$ state has a minimum very close to the middle of the FC region. This accounts for the promi-

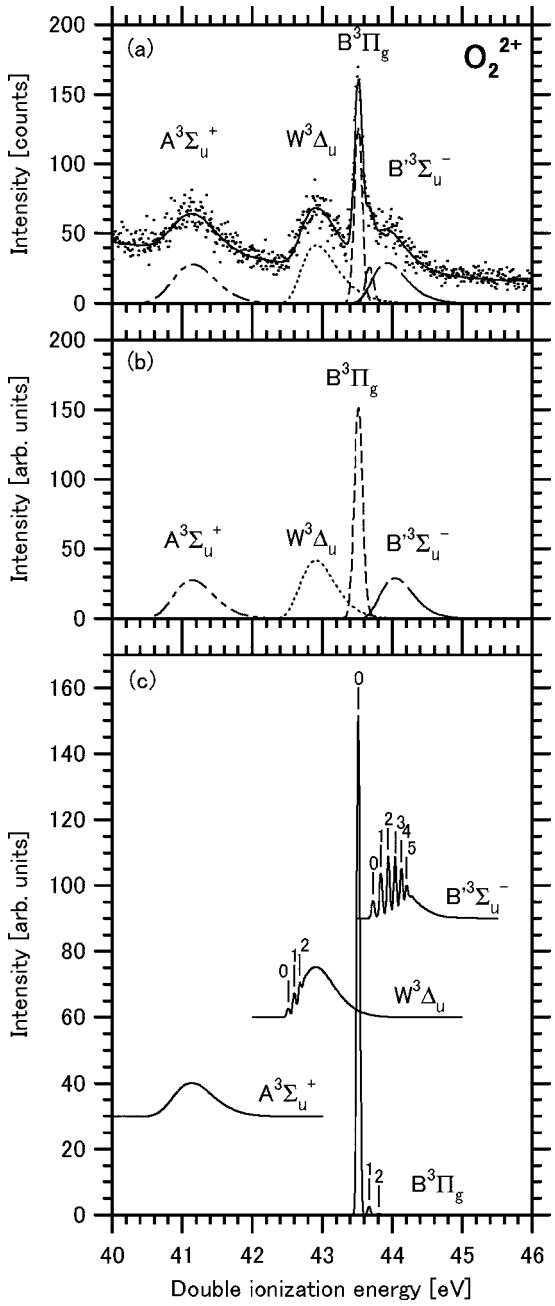

FIG. 2. (a) DCT spectrum of O_2^{2+} at 140 meV resolution. The solid line through the experimental data points is the sum of the best-fit peaks. At the bottom, the electronic states are separately shown with different types of lines: dash-two dotted ($A\ ^3\Sigma_u^+$), dotted ($W\ ^3\Delta_u$), dashed ($B\ ^3\Pi_g\ v=0,1$), and dash-dotted ($B'\ ^3\Sigma_u^-$). (b) *Ab initio* FC profiles assuming the instrumental resolution of 140 meV. Relative intensities among the electronic states, $A\ ^3\Sigma_u^+$, $W\ ^3\Delta_u$, $B\ ^3\Pi_g$, and $B'\ ^3\Sigma_u^-$, were adjusted to be 14:18.5:16.5:12 to reproduce the experimental spectrum. (c) As (b) but assuming an instrumental resolution of 50 meV. To clarify the spectral shapes, the electronic states are separately shown with different baseline values.

nence of the $v=0$ level, considering the vertical nature of DCT spectroscopy.

In contrast to the $B\ ^3\Pi_g$ state, the spectral shape of the other electronic bands, namely $A\ ^3\Sigma_u^+$, $W\ ^3\Delta_u$, and $B'\ ^3\Sigma_u^-$ states, are broad without any vibrational structure. In this case, there can be two possible reasons for the smearing of the vibrational structure. First, the corresponding dicationic state is repulsive around the FC region. Second, the dicationic state is quasibound around the FC region but the energy resolution of the spectrometer is insufficient to resolve vibrational levels. In either case, however, we can obtain information on the dicationic potential curves from the band shapes by analogy with photoelectron spectroscopy [25]. If a band shows a sharp rise at the lower-energy side, the FC factor for the $v=0$ level is sufficiently large; this means that the change of equilibrium distance during double ionization is small. On the other hand, if a band is bell-shaped, the FC factor for the $v=0$ level is negligibly small; this means that the corresponding dicationic state is weakly bound with its equilibrium distance much larger than that of the neutral ground state, or is dissociative. The band shapes of the $A\ ^3\Sigma_u^+$, $W\ ^3\Delta_u$, and $B'\ ^3\Sigma_u^-$ states are the latter case, where the potential-energy curves of these dicationic states seem to be well represented by repulsive functions within the FC region.

In order to analyze the observed band shapes quantitatively, we have assumed the following exponential functions for the potential-energy curves of the $A\ ^3\Sigma_u^+$, $W\ ^3\Delta_u$, and $B'\ ^3\Sigma_u^-$ states within the FC region,

$$E(R) = A\ \exp[-B(R-R_0)] + C, \tag{5}$$

where R_0 is the equilibrium distance of O_2 in its ground state. On the basis of the reflection approximation [26], the spectral profile of the electronic band can be described as

$$f(E) = D\ \exp\left[-\left(\frac{1}{Bw_0}\ln\frac{E-C}{A}\right)^2\right], \tag{6}$$

which is used for the fitting function of the present analyses. In this expression, w_0 is the spatial width of the probability density distribution of the $v=0$ wave function of O_2 in its ground state. Specifically, we have

$$|\Psi(R)|^2 \propto \exp\left[-\left(\frac{R-R_0}{w_0}\right)^2\right], \tag{7}$$

where $w_0=0.051\,64$ Å as obtained from the spectroscopic constants [22]. For the quasibound $B\ ^3\Pi_g$ state, the Gaussian fitting function is used including the $v=0$ and 1 levels, whose vibrational spacing $\omega=158$ meV as taken from the DFKER results [10]. The weighted least-squares fitting was applied under assuming the smooth background. The results are shown at the bottom of Fig. 2(a). The experimentally determined potential-energy curves of the $A\ ^3\Sigma_u^+$, $W\ ^3\Delta_u$, and $B'\ ^3\Sigma_u^-$ states are shown in Fig. 3.

In the previous TPESCO spectrum [11], a single peak, which was assigned to the $A\ ^3\Sigma_u^+\ v=0$ level, was observed at 41.3 eV. In the corresponding DCT spectrum, however, only a broad structure is seen with no vibrational peaks. The vertical double ionization energy (which is defined as the energy giving the band maximum) of this electronic state is determined to be 41.15 ± 0.02 eV by the present analysis. The experimentally determined potential curve is relatively steep within the FC region, as shown in Fig. 3. This is consistent with the previous *ab initio* results [10,14]; the $A\ ^3\Sigma_u^+$ state is purely repulsive. In the DFKER spectrum [10], the spectral

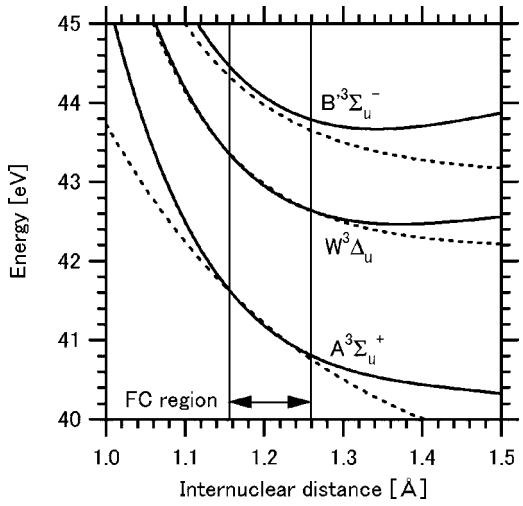

FIG. 3. Potential-energy curves of the low-lying triplet states of O_2^{2+} near the FC region. Solid lines represents the results of the present *ab initio* calculation using the aug-cc-pVQZ basis set, while broken lines represent experimentally derived potential curves assuming exponential functions (see text for details).

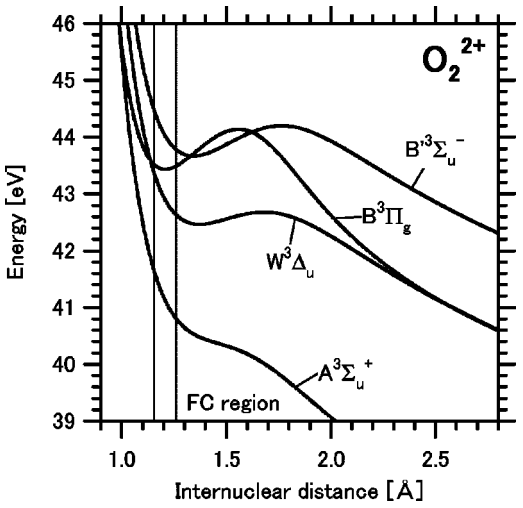

FIG. 4. Potential-energy curves of the low-lying triplet states of O_2^{2+}. The vertical energy scale is adjusted so that the $v=0$ level of the $B\ ^3\Pi_g$ state coincides with the present observation. The FC region is indicated with vertical lines.

profile of the $A\ ^3\Sigma_u^+$ state overlapped with the vibrational progression of the $1\ ^1\Sigma_u^-$ state and therefore the contribution from the $A\ ^3\Sigma_u^+$ state could not be sorted out.

The vertical double ionization energy of the $W\ ^3\Delta_u$ state is determined to be 42.92 ± 0.02 eV. In the corresponding DFKER spectrum, this band exhibits a typical profile showing a transition to both bound and repulsive parts in the final state. Its maximum lies in the repulsive part around 42.9 eV, which agrees with the present DCT observation.

As for the $B'\ ^3\Sigma_u^-$ state, five vibrational levels were resolved in the DFKER spectrum with a band maximum around $v=2$ (43.990 eV) and $v=3$ (44.093 eV). In the present DCT spectrum, only a broad feature is observed, which is due to the insufficient energy resolution of the spectrometer. The band maximum lies at 43.92 ± 0.04 eV, which is slightly lower than that observed in the DFKER spectrum. This discrepancy can be attributed to the inaccuracy of the present analysis; the error of the fitting for this state is relatively large because of the contribution of the $B\ ^3\Pi_g$ state.

C. Comparison with *ab initio* calculations

For a quantitative check of the present analyses, the potential-energy curves of the low-lying O_2^{2+} triplet states have been calculated with the full valence CASSCF-MRCI method. Figure 4 shows the potential-energy curves obtained with the largest basis set (aug-cc-pVQZ). The energy axis is adjusted so that the $B\ ^3\Pi_g\ v=0$ level coincides with the experimental energy 43.514 eV. On the whole, these potential-energy curves are similar in shape to those of previous calculations [10,14]. An expanded part of the $A\ ^3\Sigma_u^+$, $W\ ^3\Delta_u$, and $B'\ ^3\Sigma_u^-$ states around the FC region is shown in Fig. 3 to compare with the experimental results. Table II summarizes the theoretical equilibrium distances, defined as the minimum point of the potential-energy curves.

As shown in Fig. 3, the experimentally obtained potential curves of the $A\ ^3\Sigma_u^+$ and $W\ ^3\Delta_u$ states are in excellent agreement with the corresponding theoretical ones. In contrast, the agreement for the $B'\ ^3\Sigma_u^-$ state is not as good. This is attributed to the inaccuracy of the analysis, as we mentioned above.

Using the potential-energy curves with the aug-cc-pVQZ basis set, we have calculated the theoretical spectrum, i.e., the FC profiles assuming the Gaussian instrumental resolution. To compare with the present DCT spectrum, 140 meV instrumental resolution is assumed. The theoretical spectrum thus obtained is shown in Fig. 2(b). In order to confirm the accuracy of the present predictions, the theoretical spectrum is compared with the other high-resolution spectrum. To compare with the DFKER spectrum [10], 50 meV instrumental resolution is assumed. The obtained theoretical spectrum is shown in Fig. 2(c). As seen in Fig. 2(c), the vibrational levels of the $W\ ^3\Delta_u$, $B\ ^3\Pi_g$, and $B'\ ^3\Sigma_u^-$ states are predicted. The theoretical vibrational energies are summarized in Table III together with the DFKER results. As seen in this table, the agreement with respect to the positions of the vibrational levels is good.

The $A\ ^3\Sigma_u^+$ state is predicted to be purely repulsive within the whole internuclear distance by the present *ab initio* calculations; this result is the same as those obtained by the previous calculations [10,14]. The FC profile of this electronic state has a maximum at 41.14 eV [Fig. 2(b)], which is

TABLE II. Theoretical equilibrium distance in angstroms.

State	AVDZ[a]	AVTZ[b]	AVQZ[c]
$A\ ^3\Sigma_u^+$			
$W\ ^3\Delta_u$	1.4227	1.3860	1.3705
$B\ ^3\Pi_g$	1.2246	1.2155	1.2070
$B'\ ^3\Sigma_u^-$	1.3752	1.3530	1.3421

[a]Using aug-cc-pVDZ basis set.
[b]Using aug-cc-pVTZ basis set.
[c]Using aug-cc-pVQZ basis set.

TABLE III. Energies of vibrational levels of O_2^{2+} in eV.

State	v	Theory[a]	Experiment[b]
$W\ ^3\Delta_u$	0	42.514	42.531
	1	42.601	42.621
	2	42.673	42.697
$B\ ^3\Pi_g$	0	(43.514)	(43.514)
	1	43.666	43.672
	2	43.808	43.812
$B'\ ^3\Sigma_g^-$	0	43.726	
	1	43.837	43.843
	2	43.943	43.954
	3	44.040	44.057
	4	44.128	44.148
	5	44.200	

[a]Using aug-cc-pVQZ basis set. The energy scale is adjusted so that the $v=0$ level of the $B\ ^3\Pi_g$ state coincides with the present DCT observation.

[b]Previous DFKER results by Lundqvist *et al.* [10]. The energy scale is adjusted so that the $v=0$ level of the $B\ ^3\Pi_g$ state coincides with the present DCT observation.

in good agreement with the present DCT observation.

In the theoretical band of the $W\ ^3\Delta_u$ state, three vibrational peaks are predicted [Fig. 2(c)], and its maximum is located at 42.91 eV in the repulsive part of this electronic state. The whole band profile of the $W\ ^3\Delta_u$ state in the DFKER spectrum [10] is perfectly reproduced by the present *ab initio* spectrum. In contrast, the previous calculation [10] predicted only two vibrational levels in this state. This inaccuracy can be accounted for by the basis-set truncation of *ab initio* calculations because our calculation with the smaller basis set (aug-cc-pVDZ and aug-cc-pVTZ) also failed to support three vibrational levels.

According to the present *ab initio* prediction for the $B\ ^3\Pi_g$ state, most of the vibrational population goes into the $v=0$ level because the potential-energy curve of this state has a potential minimum very close to the middle of the FC region (Fig. 4 and Table II). This is consistent with previous calculations.

As for the $B'\ ^3\Sigma_u^-$ state, the whole theoretical band profile cannot be compared with that observed in the DFKER spectrum. According to the estimation of Lundqvist *et al.* [10], the $v=0$ level of this state has a fairly long lifetime toward dissociation. Consequently, the $v=0$ peak was not observed in the DFKER spectrum. Furthermore, the continuous intensity distribution part of this state overlapped with the progression of the $1\ ^1\Sigma_u^-$ state in the DFKER spectrum. However, relative intensities in the range $v=1$ to 4 are well reproduced by the present calculations [see Fig. 4 of Ref. [10] and Fig. 2(c)]. In the present predications, we can see the $v=5$ peak of this state, which is weakly discernible in the corresponding DFKER spectrum. In contrast, the previous calculation [10] predicted only four vibrational levels in this state.

On the whole, the present FC profiles reproduced well the present DCT and DFKER spectra. Comparing the FC profiles with the DCT observations in detail, however, a small discrepancy can be seen. In the present DCT spectrum, the relative intensities between the $v=0$ and 1 levels of the $B\ ^3\Pi_g$ state are 1:0.20, while our calculation predicts the relative intensities to be 1:0.02. This discrepancy is partly due to the inaccuracy of the potential-energy curves. As the larger basis set is used, the equilibrium distance of the $B\ ^3\Pi_g$ state becomes shorter (Table II). A more accurate calculation with a larger basis set will result in a shorter equilibrium length; this tends to compensate for the discrepancy considering the equilibrium distance of the neutral ground state is 1.207 52 Å. In fact, such vibrational excitation was also seen in the DFKER spectrum [10], where the relative intensities are 1:0.07. The other reason for the discrepancy still remaining can be a slight breakdown of the FC principle in DCT spectroscopy, as reported for NO^{2+} [16]. Further experimental and theoretical investigations are necessary to account for the origin of this discrepancy.

D. Possibility of luminescence due to the $B\ ^3\Pi_g \rightarrow A\ ^3\Sigma_u^+$ transition

From the present results, the possibility for observing the luminescence due to the $B\ ^3\Pi_g \rightarrow A\ ^3\Sigma_u^+$ transition can be discussed. In the luminescence spectrum of Tohji *et al.* [12], three vibrational peaks were resolved. For such vibrational progression to be observed, both the $B\ ^3\Pi_g$ and $A\ ^3\Sigma_u^+$ states must be quasibound with their equilibrium distance close to each other. According to the present results, however, the equilibrium distance of the $B\ ^3\Pi_g$ state lies close to the middle of the FC region, while the potential-energy curve of the $A\ ^3\Sigma_u^+$ state is repulsive within the FC region.

Still there is a possibility for the luminescence due to the $B\ ^3\Pi_g \rightarrow A\ ^3\Sigma_u^+$ by the bound-free transition. We have estimated the peak width due to the bound-free transition by the wave-packet method. In this case, the initial wave packet is the $v=0$ vibrational wave function of the $B\ ^3\Pi_g$ state. The initial wave packet was put on the potential curve of the $A\ ^3\Sigma_u^+$ state at the equilibrium distance of the $B\ ^3\Pi_g$ state, and the time propagation of the wave packet is examined. Because the vibrational frequency and the equilibrium distance of the $B\ ^3\Pi_g$ state (1420 cm^{-1} [10], 1.2070 Å) do not differ much from those of the O_2 ground state (1580.19 cm^{-1}, 1.207 52 Å [22]), the estimated peak width is broad ($\approx$0.6 eV), similar to the profile of the $A\ ^3\Sigma_u^+$ state in Fig. 2(c). This peak width is much wider than that observed in the luminescence spectrum by Tohji *et al.* Thus, the present results cast doubt on the previous assignment of the luminescence to the $O_2^{2+}\ B\ ^3\Pi_g \rightarrow A\ ^3\Sigma_u^+$ transition.

V. CONCLUSION

We have observed the DCT spectrum of O_2^{2+}. From the shape of the band structure, the potential-energy curves of the $A\ ^3\Sigma_u^+$, $W\ ^3\Delta_u$, and $B'\ ^3\Sigma_u^-$ states within the FC region are experimentally determined based on the reflection approximation. The potential-energy curves experimentally derived are compared with those obtained by the full valence CASSCF-MRCI calculations. The theoretical potential-

energy curve of the $A\ ^3\Sigma_u^+$ state is identical with that obtained by the present experiment; the $A\ ^3\Sigma_u^+$ state is repulsive near the FC region. As for the $B\ ^3\Pi_g$ state, the theoretical potential well is very close to the middle of the FC region; this accounts for the prominence of the $v=0$ level in the present DCT spectrum. These results cast doubt on the previous assignment of luminescence to the $O_2^{2+}\ B\ ^3\Pi_g \rightarrow A\ ^3\Sigma_u^+$ transition [12]. The potential-energy curve of the $A\ ^3\Sigma_u^+$ state obtained by the present *ab initio* calculation is purely repulsive within the whole internuclear distance, in agreement with other theoretical works [10,14]. The present result does not support the observed bound level of the $A\ ^3\Sigma_u^+$ state by the previous TPESCO experiment [11].

Although the energy resolution is less perfected in comparison with the TPESCO and DFKER methods, DCT spectra directly reflect the vertical transition from the ground state of a neutral molecule to the corresponding dicationic states. According to this simple interpretation, we could demonstrate for O_2^{2+} that DCT spectroscopy has a unique opportunity to study molecular dications.

ACKNOWLEDGMENT

This research was partially supported by the Ministry of Education, Science, Sports, and Culture of Japan, Grant-in-Aid for Young Scientists (B), 2004, 16740234.

[1] J. H. D. Eland, S. S. W. Ho, and H. L. Worthington, Chem. Phys. **290**, 27 (2003).
[2] D. Mathur, Phys. Rep. **225**, 193 (1993).
[3] S. S. Prasad and D. R. Furman, J. Geophys. Res. **80**, 1360 (1975).
[4] M. Larsson, P. Baltzer, S. Svensson, B. Wannberg, N. Martensson, A. N. de Brito, N. Correia, M. P. Keane, M. Carlsson-Gothe, and L. Karlsson, J. Phys. B **23**, 1175 (1990).
[5] J. Fournier, P. G. Fournier, M. L. Langford, M. Mousselmal, J. M. Robbe, and G. Gandara, J. Chem. Phys. **96**, 3594 (1992).
[6] M. Hamdan and A. G. Brenton, Chem. Phys. Lett. **164**, 413 (1989).
[7] D. M. Curtis and J. H. D. Eland, Int. J. Mass Spectrom. Ion Processes **63**, 241 (1985).
[8] S. D. Price and J. H. D. Eland, J. Phys. B **24**, 4379 (1991).
[9] R. I. Hall, G. Dawber, A. McConkey, M. A. MacDonald, and G. C. King, Phys. Rev. Lett. **68**, 2751 (1992).
[10] M. Lundqvist, D. Edvardsson, P. Baltzer, M. Larsson, and B. Wannberg, J. Phys. B **29**, 499 (1996).
[11] G. Dawber, A. G. McConkey, L. Avaldi, M. A. MacDonald, G. C. King, and R. I. Hall, J. Phys. B **27**, 2191 (1994).
[12] K. Tohji, D. M. Hanson, and B. X. Yang, J. Chem. Phys. **85**, 7492 (1986).
[13] A. C. Hurley, J. Mol. Spectrosc. **9**, 18 (1962).
[14] L. G. M. Pettersson and M. Larsson, J. Chem. Phys. **94**, 818 (1991).
[15] O. Furuhashi, T. Kinugawa, S. Masuda, C. Yamada, and S. Ohtani, Chem. Phys. Lett. **337**, 97 (2001).
[16] O. Furuhashi, T. Kinugawa, T. Hirayama, T. Koizumi, C. Yamada, and S. Ohtani, Chem. Phys. **295**, 185 (2003).
[17] J. Appell, *Collision Spectroscopy* (Plenum Press, New York, 1978), Chap. 4.
[18] NIST Atomic Spectra Database Levels Form. http://physics.nist.gov/cgi-bin/AtData/levels_form
[19] MOLPRO (Version 2000.1) is a package of *ab initio* programs written by H.-J. Werner and P. J. Knowles, with contributions from R. D. Amos *et al.*
[20] R. A. Kendall, T. H. Dunning, and R. J. Harrison, J. Chem. Phys. **96**, 6796 (1992).
[21] S. R. Langhoff and E. R. Davidson, Int. J. Quantum Chem. **8**, 61 (1974).
[22] K. P. Huber and G. Herzberg, *Molecular Spectra and Molecular Structure. IV. Constants of Diatomic Molecules* (Van Nostrand–Reinhold, New York, 1979).
[23] E. J. Heller, J. Chem. Phys. **68**, 2066 (1978).
[24] M. D. Feit, J. A. Fleck, and A. Steiger, J. Comput. Phys. **47**, 412 (1982).
[25] J. H. D. Eland, *Photoelectron Spectroscopy* (Butterworth, London, 1974).
[26] G. Herzberg, *Molecular Spectra and Molecular Structure. I. Spectra of Diatomic Molecules* (Van Nostrand–Reinhold, New York, 1950).